Products of the addition of water molecules to $Al_3O_3^-$ clusters: Structure, bonding, and electron binding energies in $Al_3O_4H_2^-$, $Al_3O_5H_4^-$, $Al_3O_4H_2$, and $Al_3O_5H_4$

Francisco J. Tenorio
Department of Chemistry, Kansas State University, Manhattan, Kansas 66506-3701 and Facultad de Química, Universidad de Guanajuato, Noria Alta s/n, Guanajuato, GTO, 36050, México

Ian Murray
Department of Chemistry, Kansas State University, Manhattan, Kansas 66506-3701

Ana Martínez
Instituto de Investigaciones en Materiales, UNAM, Circuito Exterior s/n, C. U., P.O. Box 70-360, Coyoacán, 04510, D.F. México

Kenneth J. Klabunde and J. V. Ortiz[a)]
Department of Chemistry, Kansas State University, Manhattan, Kansas 66506-3701

(Received 5 December 2003; accepted 3 February 2004)

Two stable products of reactions of water molecules with the $Al_3O_3^-$ cluster, $Al_3O_4H_2^-$ and $Al_3O_5H_4^-$, are studied with electronic structure calculations. There are several minima with similar energies for both anions and the corresponding molecules. Dissociative absorption of a water molecule to produce an anionic cluster with hydroxide ions is thermodynamically favored over the formation of $Al_3O_3^-(H_2O)_n$ complexes. Vertical electron detachment energies of $Al_3O_4H_2^-$ and $Al_3O_5H_4^-$ calculated with *ab initio* electron propagator methods provide a quantitative interpretation of recent anion photoelectron spectra. Contrasts and similarities in these spectra may be explained in terms of the Dyson orbitals associated with each transition energy. © *2004 American Institute of Physics.* [DOI: 10.1063/1.1689648]

I. INTRODUCTION

Aluminum oxide reactivity is a common concern of industrial and environmental scientists.[1] With the advent of synthetic techniques that control particle size and stoichiometry, basic investigations of the reactivity of aluminum oxides now may consider interactions between individual reagent molecules and specific Al_nO_m clusters. Reactions involving water molecules are especially important, for hydroxyl groups have a crucial effect on the surface chemistry of aluminum oxides.[2] Electronic structure underlies these elementary reactive properties; aluminum oxide and hydroxide clusters therefore have been examined in the gas phase with several spectroscopic techniques.[3–10]

Anion photoelectron spectra[4–9] and their theoretical interpretations[11–19] have demonstrated the importance of isomerism in anionic and neutral clusters that consist of aluminum and oxygen atoms. Relationships between coordination environments, electron binding energies, and charge distributions also have been established.[14–17] Recent evidence of photoisomerization by $Al_3O_3^-$ (Ref. 6) has stimulated additional experimental[7,8] and theoretical[18,19] study.

Reactions between $Al_3O_3^-$ and water molecules have been examined with mass spectrometry and the products have been characterized with anion photoelectron spectroscopy.[8] With the former technique, the presence of species with the formula $Al_3O_3^-(H_2O)$ or $Al_3O_3^-(H_2O)_2$, the relative abundance of the latter cluster, and the absence of $Al_3O_3^-(H_2O)_n$ species for $n \geqslant 3$ have been noted for moderate water vapor pressures. Anion photoelectron spectra are qualitatively different for the $n=1$ cluster with respect to the $n=0$ and 2 cases. These results suggest that electronic structure is markedly different in $Al_3O_4H_2^-$ and that $Al_3O_3^-$ and $Al_3O_5H_4^-$ have common qualitative features.

Electron propagator theory provides a framework for the systematic inclusion of electron correlation in a one-electron picture of molecular electronic structure.[20] Propagator calculations produce Dyson orbitals and correlated electron binding energies without many-body wave functions or energies of individual states. Several approximate propagators have been shown to be accurate and efficient tools for the computation of vertical and adiabatic electron binding energies. The association of Dyson orbitals to these transition energies facilitates interpretation of chemical bonding in terms of one-electron concepts.

In previous works, we have reported the ground-state geometries and energies of the low-lying states of neutral and anionic clusters with the formula Al_3O_n, where $n=1-5$ (Refs. 14–17). Electron propagator calculations on vertical electron detachment energies (VEDEs) were used to assign anion photoelectron spectra. Localization patterns in the Dyson orbitals provided an improved understanding of relationships between electron binding energies and coordi-

a)Electronic mail: ortiz@ksu.edu

nation environments. For the $Al_3O_3^-$ cluster, the existence of approximately isoenergetic book (also known as box[14,16]) and kite isomers was demonstrated by assigning calculated VEDEs of both isomers to peaks in the photoelectron spectrum.[13,14,16] A low-energy peak whose intensity varies with ion source conditions was in close agreement with the lowest calculated VEDE of the less stable kite isomer.

This work is a study of neutral and anionic species with $Al_3O_4H_2$ and $Al_3O_5H_4$ formulas. Optimized structures, relative energies, electron binding energies, and corresponding Dyson orbitals are reported. An interpretation of the photoelectron spectra of $Al_3O_4H_2^-$ and $Al_3O_5H_4^-$ also is presented.

II. METHODS

All calculations have been done with the GAUSSIAN 98 program.[21] Full geometry optimization without symmetry constraints was performed using B3LYP (Ref. 22) density functional (DF) calculations. Optimized minima were verified with harmonic frequency analysis. To locate distinct minima on potential energy surfaces, optimizations have been started from many, initial geometries. Two kinds of anionic structures have been examined. In the first, anion–molecule complexes comprising one of the two most stable structures of $Al_3O_3^-$ (book or kite) and a water molecule were optimized with the 6-311+G(2d,p) basis set.[23] Initial nuclear geometries were designed to encounter minima with dative interactions between water oxygen atoms and cationic aluminum centers or hydrogen bonds between water protons and oxide centers in $Al_3O_3^-$. The second kind assumes dissociative absorption of one or two molecules of H_2O, where hydroxide ions and protons are added to $Al_3O_3^-$. The 6-311G** basis was used for preliminary optimizations. Some initial structures were based on the most stable isomers of $Al_3O_4^-$ (Ref. 17) and $Al_3O_5^-$ (Ref. 15), where two or four hydrogen atoms are attached, respectively, to oxides to form hydroxide ions. Optimizations on the corresponding neutral doublets also were performed. The most stable anionic structures from DF calculations were reexamined with additional geometry optimizations, first with the larger 6-311++G(2df,2p) basis set[23] at the B3LYP level and, subsequently, at the MP2 level, with the 6-311G** basis set. No substantial structural differences between these results were found; discrepancies between bond lengths were less than 0.001 nm.

MP2/6-311G** geometries were employed in correlated, *ab initio*, electron propagator calculations of the VEDEs of the anions with the 6-311++G(2df,2p) basis set. The P3 (Refs. 24 and 25) and OVGF (Refs. 26 and 27) electron propagator approximations were compared in preliminary calculations, and the former method produces first and second VEDEs for the three lowest isomers of $Al_3O_4H_2^-$ that are approximately 0.2 eV lower than those of the latter method. P3 results are somewhat more accurate than those of OVGF for the first two VEDEs of $Al_3O_3^-$. The lower requirements for arithmetic operations and integral storage in the P3 method therefore recommend its employment in calculations on $Al_3O_4H_2^-$ and $Al_3O_5H_4^-$.

For each VEDE calculated with electron propagator methods, there corresponds a Dyson orbital defined by

$$\Phi^{\mathrm{Dyson}}(x_1) = N^{-1/2} \int \Psi_{\mathrm{anion}}(x_1, x_2, x_3, \ldots, x_N) \times \Psi^*_{\mathrm{neutral}}(x_2, x_3, x_4, \ldots, x_N) dx_2 dx_3 dx_4 \cdots dx_N,$$

where N is the number of electrons in the anion and x_i is the space-spin coordinate of the ith electron.[20] The Dyson orbital represents the change in electronic structure accompanying the detachment of an electron from an anion. Dyson orbitals corresponding to each VEDE in the P3 approximation are proportional to canonical, Hartree–Fock orbitals. Pole strengths, which are equal to the integral over all space of the absolute value squared of the Dyson orbital, are indices of the validity of perturbative electron propagator calculations that are based on canonical, Hartree–Fock orbital energies and the results of Koopmans's theorem. When pole strengths lie between 0.85 and unity, these approximations are validated.

Contour plots of normalized Dyson orbitals were generated with the MOLDEN program.[28] The contour values represented in the plots are ± 0.03.

III. STRUCTURES

A. Anion–molecule complexes

Geometry optimizations for complexes with the formula $Al_3O_3^-(H_2O)$ were initiated from structures with (a) close H_2O–Al, donor–acceptor interactions, (b) a hydrogen bond between the water molecule and an anion oxide center, or (c) both kinds of interactions. An exhaustive series of optimizations was performed for this kind of species. The most stable anion–molecule structures anticipate the two lowest isomers of $Al_3O_4H_2^-$ (see below).

For the book form of $Al_3O_3^-$, the water molecule's oxygen atom approaches the central aluminum atom and a partial closing of the book about its spine (that is, closing of the dihedral angle about the central Al–O bond axis) takes place. Previous studies[14–17] have shown that aluminum-rich clusters, where the Al:O stoichiometric ratio exceeds two-thirds, have occupied orbitals distributed chiefly over the aluminum atoms with the smallest number of oxygen neighbors. Since the central aluminum atom has the largest number of oxygen neighbors, the four least-bound electrons are distributed over the two noncentral aluminum atoms in $Al_3O_3^-$. Therefore, the central aluminum atom is the most positively charged and is the best site for the approach of the water molecule's lone pairs. In the kite isomer of $Al_3O_3^-$, the central aluminum atom has the highest number of oxygen neighbors and it therefore has the highest positive charge. Lone pairs on the water oxygen atom coordinate to this center while a proton is bent toward the oxygen atom on the tail of the kite anion.

Both of these anion–molecule structures have energies that are approximately 35 kcal/mol above those of the most stable clusters in the following section. Additional optimizations encounter many other, less-stable anion–molecule minima. It is unlikely that any of these complexes is represented in the photoelectron spectra of $Al_3O_4H_2^-$.

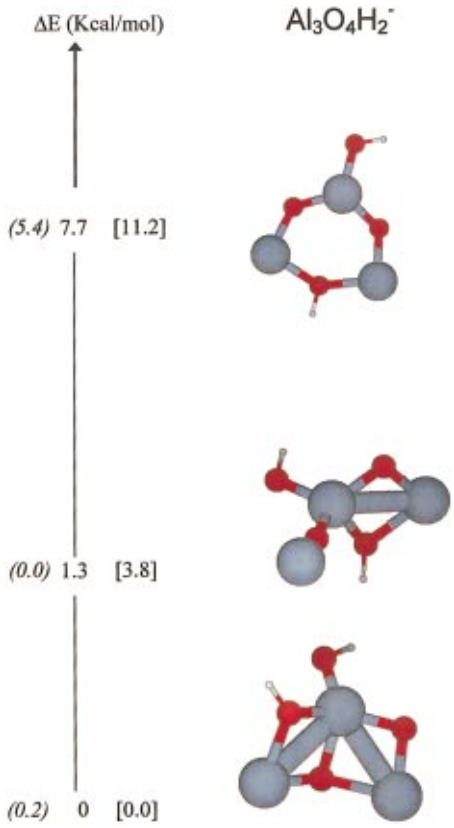

FIG. 1. (Color) B3LYP/6-311G** structures and relative energies of $Al_3O_4H_2^-$. Here B3LYP/6-311G++G(2df,2p) and MP2/6-311G** relative energies are listed in parentheses and brackets, respectively.

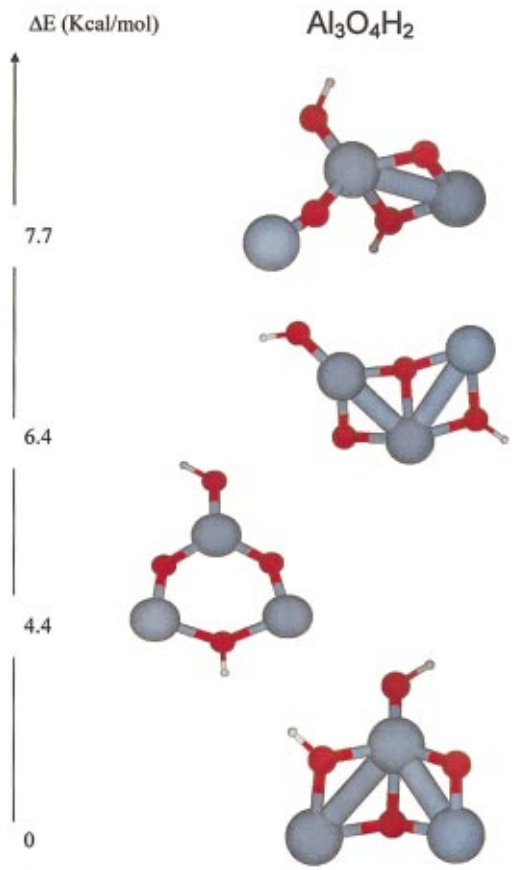

FIG. 2. (Color) B3LYP/6-311G** structures and relative energies of $Al_3O_4H_2$.

B. $Al_3O_4H_2^-$ and $Al_3O_4H_2$

The most stable anionic and neutral structures are shown in Figs. 1 and 2, respectively, along with their relative energies. B3LYP/6-311G** values lie on the vertical axis; B3LYP/6-311++G(2df,2p) and MP2/6-311G** values are listed in parentheses and brackets, respectively. Two, anionic, C_1 minima lie very close to each other in energy. The first is similar to the booklike structure that was obtained previously for $Al_3O_3^-$ (Refs. 13, 14, and 16). Here, in contrast, a hydroxide is coordinated to the central Al atom and a proton has been added to a neighboring oxide center. The second resembles the C_{2v}, kitelike structure obtained in the same work on $Al_3O_3^-$, for there are four-member rings with two aluminum atoms and two oxygen atoms in both structures. In contrast, the $Al_3O_4H_2^-$ structure's central aluminum has four neighbors in an approximately tetrahedral arrangement instead of three neighbors in a trigonal, planar geometry. The same aluminum atom has a hydroxide ligand and one of the ring oxygens now has a covalently bonded hydrogen. In addition, there is a planar structure with a six-member ring that is 7.7 kcal/mol higher in energy than the first isomer. Such instability implies that the corresponding anion is unlikely to contribute significantly to the features in the photoelectron spectrum. At this level of calculation, the energy difference between the two lowest structures is not large enough to definitively determine which isomer is the more stable. While all three methods agree that the ring anion is least stable, there are discrepancies in the order of the book and kite species.

Relative energies of neutral structures at the B3LYP/6-311G** level are shown in Fig. 2. The most stable structure resembles its anionic counterpart, but the order of the less stable neutral isomers is not the same as that for the anion. In addition to the ring and kite isomers found in Fig. 1, there is another book structure where a terminal hydroxide is coordinated to a noncentral aluminum atom. The ring isomer is the second most stable form. Another isomer, not shown in Fig. 2, lies at 7.4 kcal/mol and has an open-chain, Al–O–Al–O–$Al(OH)_2$ structure.

C. $Al_3O_5H_4^-$ and $Al_3O_5H_4$

The lowest isomers for $Al_3O_5H_4^-$ and $Al_3O_5H_4$ and their relative energies are shown in Figs. 3 and 4, respectively. The most stable structure of this anion also resembles the booklike isomer of $Al_3O_3^-$, but there are several important differences. The central aluminum now has two hydroxide ligands and the two neighboring oxygen atoms have become hydroxides, in agreement with a structure suggested by Akin and Jarrold.[8] In addition, the central core of three aluminum and three oxygen atoms is no longer planar. Forcing C_{2v} symmetry results in a second-order saddle point. Whereas rotation barriers about O–H bonds in the hydroxides coordinated to the central aluminum atom are likely to

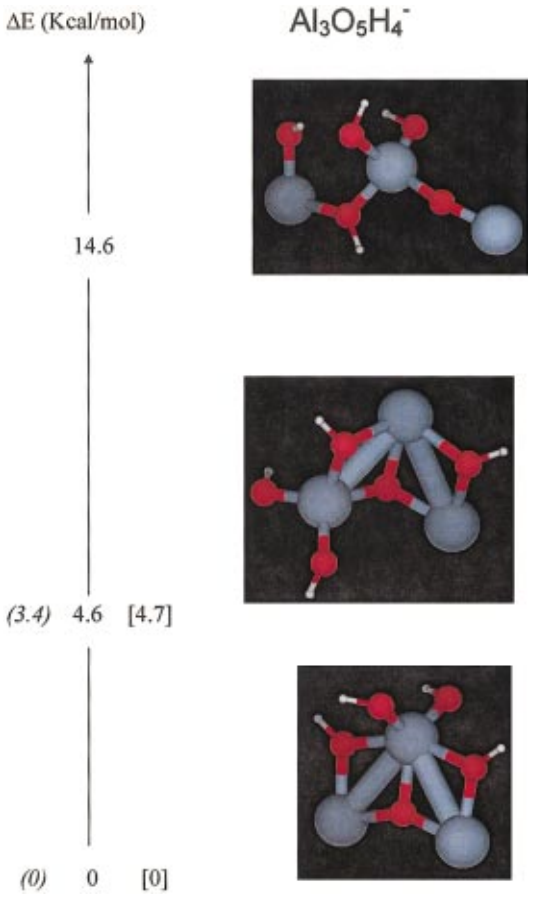

FIG. 3. (Color) B3LYP/6-311G** structures and relative energies of $Al_3O_5H_4^-$. Here B3LYP/6-311G++G(2df,2p) and MP2/6-311G** relative energies are listed in parentheses and brackets, respectively.

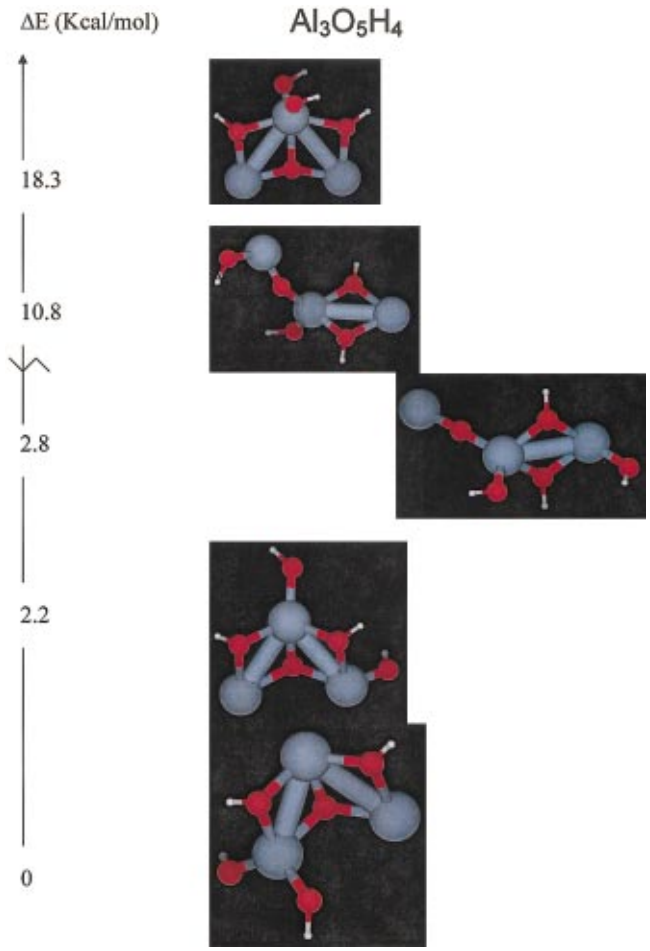

FIG. 4. (Color) B3LYP/6-311G** structures and relative energies of $Al_3O_5H_4$.

be low, there is an approximate symmetry relationship between the noncentral aluminum atoms, between the bridging hydroxides, and between the terminal hydroxides. Therefore, the most stable isomer is designated the symmetric book structure, for the symmetric, booklike framework found in $Al_3O_3^-$ is preserved approximately. In the second most stable structure, two hydroxides are coordinated to a noncentral aluminum atom. The same oxygen atoms that constitute bridges between the central and noncentral aluminum atoms are protonated in both isomers. The second structure's relative energy is low enough to warrant consideration when interpreting the photoelectron spectrum of $Al_3O_5H_4^-$. Whereas this isomer also retains the booklike framework of $Al_3O_3^-$, it is designated the asymmetric book structure. An open structure, shown in Fig. 3, is considerably less stable than the other two. A recent computational study also reports an isomer at 11 kcal/mol that is based on a kite structure.[19] All three total energy procedures agree on the order of the two lowest anionic structures.

The order of isomers is completely different for the neutral structures displayed in Fig. 4. The lowest neutral isomer resembles the second most stable anionic structure, for both have two hydroxides coordinated to a noncentral aluminum atom. In the second most stable structure, the central aluminum atom and a noncentral aluminum atom have terminal hydroxide ligands. The anionic counterpart of this species is not among the most stable anionic structures. Whereas the two most stable neutral structures retain the Al_3O_3 booklike core, the third structure resembles the kite Al_3O_3 isomer. A four-member ring comprising two aluminum sites and two oxygen bridges and an OAI tail are found in this isomer. Both bridging oxygens are protonated; two hydroxides are coordinated to the two ring aluminum atoms. When the hydroxide coordinated to the terminal, ring aluminum atom is moved to the aluminum atom of the tail, a fourth isomer is produced which is considerably less stable than the first three isomers. The neutral counterpart of the lowest anionic structure is the least stable of the structures shown in Fig. 4.

IV. VERTICAL IONIZATION ENERGIES AND DYSON ORBITALS

Electron propagator calculations of VEDEs were performed at the geometries obtained in MP2/6-311G** optimizations. All pole strengths were between 0.89 and 0.93.

A. $Al_3O_4H_2^-$

Table I displays Koopmans and P3 results for the book VEDEs. Correlation and relaxation corrections approximately cancel for the first two final states. Final-state, orbital

TABLE I. VEDEs (eV) for the most stable isomers of $Al_3O_4H_2^-$.

Isomer	Koopmans	P3	Experiment[a]
Book	2.70	2.72	2.7–2.8
	3.79	3.78	3.8–4.0
	7.66	6.52	
	8.08	6.80	
Kite	2.95	2.99	2.7–2.8
	5.12	5.21	
	7.38	6.25	
	7.99	6.70	
Ring	2.61	2.63	2.7–2.8
	3.45	3.49	3.8–4.0
	8.59	7.30	
	8.64	7.45	
	8.96	7.75	

[a]Reference 8.

relaxation effects are larger for the next two VEDEs; discrepancies between Koopmans and P3 results exceed 1 eV in both cases.

Dyson orbitals corresponding to the two lowest VEDEs, shown in Fig. 5, consist chiefly of 3*s* functions on the noncentral aluminum atoms. For the Dyson orbital that belongs to the lowest VEDE, the largest contribution is on the aluminum coordinated to two oxides. A smaller contribution with the opposite phase is made by the 3*s* orbital on the other noncentral aluminum, which has a neighboring hydroxide bridge. In the next Dyson orbital, the latter aluminum's 3*s* function makes the largest contribution and there is some delocalization, with the same phase, into the 3*s* function of the other noncentral aluminum atom. In both Dyson orbitals, there are significant antibonding interactions with neighboring oxygen 2*p* functions. Dyson orbitals that correspond to higher VEDEs consist chiefly of oxygen 2*p* functions in antibonding relationships; aluminum contributions in these orbitals are relatively small.

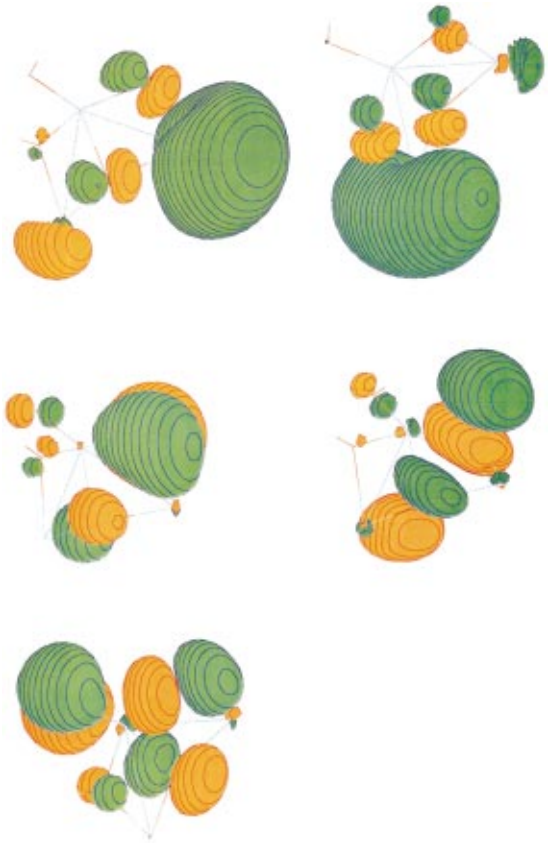

FIG. 5. (Color) Dyson orbitals for the first (top left), second (top right), third (middle left), fourth (middle right), and fifth (bottom left) VEDEs of the book isomer of $Al_3O_4H_2^-$.

Dyson orbitals for the first two VEDES of the C_{2v}, book form of $Al_3O_3^-$ consist chiefly of symmetry-adapted combinations of 3*s* functions on the two noncentral aluminum atoms. In $Al_3O_4H_2^-$, these two functions are subject to distinct electrostatic potentials and delocalization between them therefore is less pronounced. The corresponding Dyson orbitals in the book form of $Al_3O_4H_2^-$ are localized on one noncentral aluminum atom or the other. In agreement with qualitative rules deduced from previous calculations on $Al_3O_n^-$ clusters,[16] the least bound electrons are localized on the aluminums with the lowest coordination number. In the Dyson orbital of the second VEDE of $Al_3O_4H_2^-$, the more stable of the two 3*s* functions is stabilized further by a weak bonding relationship with the less stable 3*s* function. As a consequence, the latter function is destabilized by a similarly weak antibonding interaction between the two functions in the Dyson orbital of the first VEDE.

Koopmans and P3 predictions of VEDEs for the kite isomer, also shown in Table I, are close for the first two final states. Orbital relaxation effects in the final states are larger for the next two cases.

Dyson orbitals for the first four VEDEs have close relationships with their counterparts for the kite isomer of $Al_3O_3^-$. Figure 6 displays these orbitals. Localization on the aluminum with two oxygen neighbors characterizes the Dyson orbital for the lowest VEDE. In the next Dyson orbital, localization occurs on the tail aluminum atom. Antibonding relationships with neighboring oxygen 2*p* functions are present in both cases. The third and fourth Dyson orbitals exhibit, respectively, π and σ antibonding relationships between the bridging oxygen atoms; aluminum contributions are negligible in these orbitals. Comparison with the Dyson orbitals for the VEDEs of the kite form of $Al_3O_3^-$ shows little change in the aluminum-localized cases, except for the altered positions of the nuclei. In the oxygen-localized Dyson orbitals, there are larger amplitudes on the bridging hydroxide's oxygen atom than on the bridging oxide. There is also some delocalization onto the nonbridging oxygen atoms.

Patterns established in the first two isomers are repeated in the results of Table I for the ring anion. Relatively small corrections from P3 calculations to Koopmans results are found for the first two VEDEs, but orbital relaxation effects are larger for the subsequent cases.

Dyson orbitals in Fig. 7 for the first two VEDEs are composed chiefly of antisymmetric or symmetric combinations of 3*s* functions on the two aluminums with only two oxygen neighbors. Antibonding relationships with oxygen functions are present also. Dyson orbitals for higher VEDEs are centered on bridging oxygens and have minor aluminum contributions.

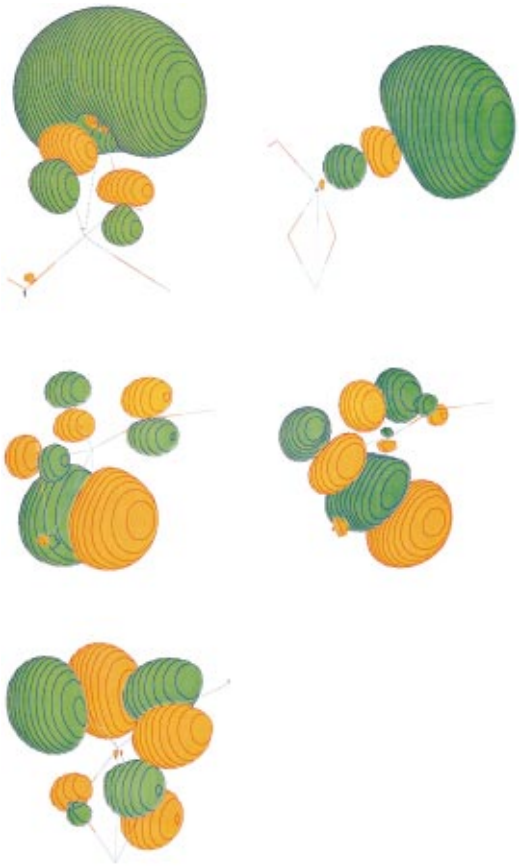

FIG. 6. (Color) Dyson orbitals for the first (top left), second (top right), third (middle left), fourth (middle right), and fifth (bottom left) VEDEs of the kite isomer of $Al_3O_4H_2^-$.

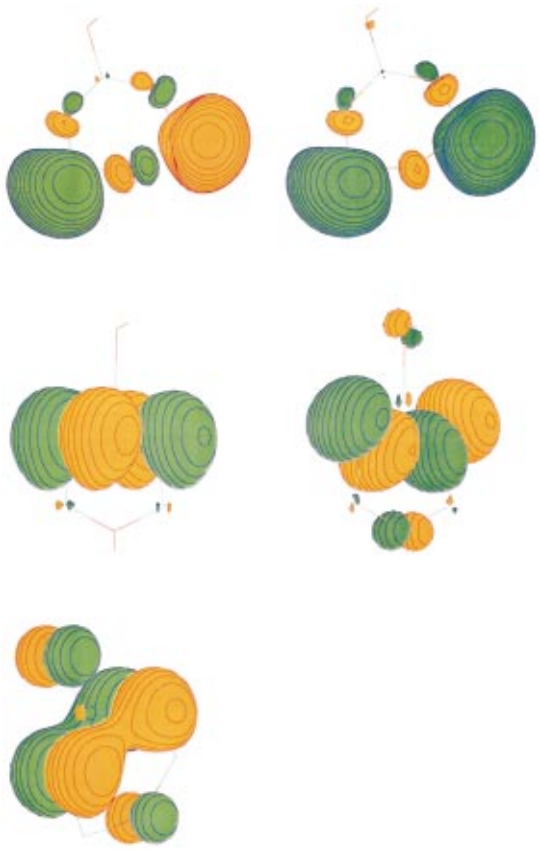

FIG. 7. (Color) Dyson orbitals for the first (top left), second (top right), third (middle left), fourth (middle right), and fifth (bottom left) VEDEs of the ring isomer of $Al_3O_4H_2^-$.

B. $Al_3O_5H_4^-$

Calculated VEDEs for the symmetric book form of $Al_3O_5H_4^-$ are given in Table II. P3 corrections to Koopmans results are approximately 0.1 eV for the first two VEDEs, but the same corrections are much larger (approximately 1.5 eV) for the remaining cases. The difference between the first two VEDEs is much smaller here than it is in the $Al_3O_4H_2^-$ clusters.

Dyson orbitals corresponding to the first two VEDEs bear a striking resemblance to their counterparts for $Al_3O_3^-$, despite the formal lack of symmetry (see Fig. 8). Noncentral aluminum 3*s* functions dominate; smaller, antibonding contributions from bridging oxygen 2*p* functions also are present. An out-of-phase relationship between 3*s* functions obtains for the first VEDE's Dyson orbital and an in-phase relationship is found in the next Dyson orbital. For the higher VEDEs, the Dyson orbitals are dominated by oxygen 2*p* functions on the nonbridging hydroxides.

Delocalization between the noncentral aluminum 3*s* functions is restored by the approximate equivalence of the electrostatic potentials at these sites. Changes in the positions of the terminal hydroxides' protons produced by rotations about the nearest O–Al bonds have little effect on this approximate symmetry relationship.

Somewhat larger P3 corrections to Koopmans results for the first two VEDEs also are seen in Table II, where predictions for the asymmetric book form are listed. Orbital relaxation effects are larger for the next two final states.

Dyson orbitals in Fig. 9 for the first two VEDEs again are delocalized between two aluminum 3*s* functions. Contributions from the four-coordinate aluminum are negligible. For the lowest VEDE, the corresponding Dyson orbital's largest contribution is made by the 3*s* function on the aluminum with three neighboring oxygen bridge atoms. There is a significant, antibonding contribution from the two-coordinate aluminum's 3*s* function. In the Dyson orbital belonging to the second VEDE, the same two functions are involved in an in-phase relationship and the larger contribution is made by the 3*s* function on the aluminum with fewer oxygen neighbors. Dyson orbitals for the third and fourth

TABLE II. VEDEs (eV) for the most stable isomers of $Al_3O_5H_4^-$.

Structure	Koopmans	P3	Experiment[a]
Symmetric book	3.34	3.23	3.3
	3.74	3.63	3.8
	8.31	6.81	
	8.96	7.48	
	9.17	7.63	
Asymmetric book	2.48	2.32	3.3
	3.77	3.64	3.8
	9.17	7.58	
	9.22	7.70	

[a]Reference 8.

FIG. 8. (Color) Dyson orbitals for the first (top left), second (top right), third (middle left), fourth (middle right), and fifth (bottom left) VEDEs of the symmetric book isomer of $Al_3O_5H_4^-$.

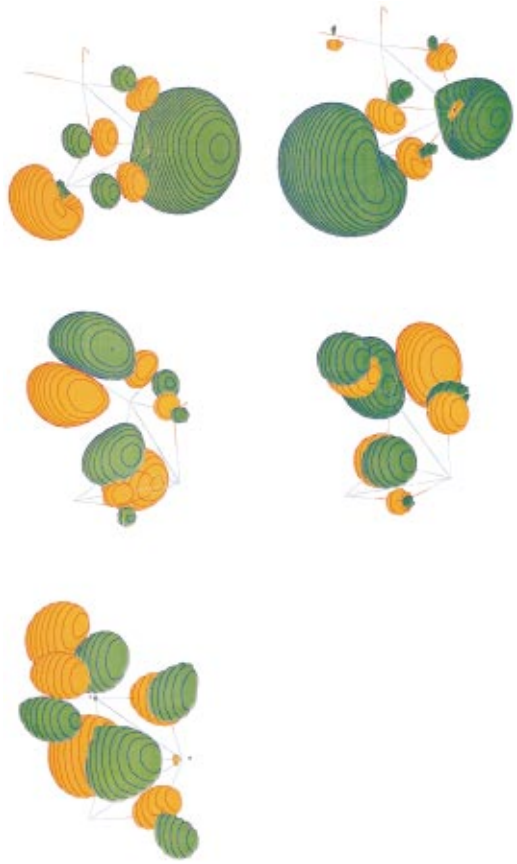

FIG. 9. (Color) Dyson orbitals for the first (top left), second (top right), third (middle left), fourth (middle right), and fifth (bottom left) VEDEs of the asymmetric book isomer of $Al_3O_5H_4^-$.

VEDEs consist chiefly of oxygen $2p$ functions on the terminal hydroxides—that is, where the lowest number of aluminum neighbors obtains.

Despite the retention of the booklike core of $Al_3O_3^-$, the pattern of localization in the first two Dyson orbitals is distinct. The least bound electrons are found on the aluminum atoms with the lowest number of oxygen neighbors. Attachment of two hydroxide groups to one of the noncentral aluminum atoms displaces electrons from this region to the central aluminum atom.

V. INTERPRETATION OF ANION PHOTOELECTRON SPECTRA

VEDEs below 4.66 eV have been inferred from photoelectron spectra of $Al_3O_3^-$, $Al_3O_4H_2^-$, and $Al_3O_5H_4^-$ (Ref. 8). In simulations of the first experiment, the origins of two peaks assigned to the book isomer are set to 2.894(10) and 3.594(9) eV. For the purpose of comparison with results discussed above, P3 calculations on $Al_3O_3^-$ were performed with the 6-311+G(2df) basis; the VEDE results are 2.85 and 3.49 eV, respectively. In a previous experimental report,[6] the corresponding values are 2.96 and 3.7 eV. Another feature with relatively low intensity has an onset near 2.2 eV and has been assigned to the kite isomer. Higher VEDEs for the kite occur near 5.2 eV and therefore are not observed with 4.66 eV radiation.

Whereas two well-separated peaks occur in the $Al_3O_3^-$ spectrum, the $Al_3O_4H_2^-$ experiment yields a more subtle pair of broad, overlapping humps. In the 4.66-eV spectrum, increases in the signal occur at 2.5 and 3.6 eV. One of the humps appears to be centered at 2.7–2.8 eV, while the other's center is located in the 3.8–4.0 eV range. Vibrational structure is not resolved in either the 4.66- or 3.49-eV spectrum.

These results are compatible with the data of Table I and suggest that the book form of $Al_3O_4H_2^-$ is chiefly responsible for the main features of the corresponding anion photoelectron spectrum. Lower symmetry in this isomer accounts for the qualitative differences between the $Al_3O_3^-$ and $Al_3O_4H_2^-$ spectra. According to the data of Fig. 1, the kite isomer is too close in energy to the book isomer to ignore. Its predicted first VEDE of 2.99 eV and the precedent of two isomers being represented in the photoelectron spectrum of $Al_3O_3^-$ suggest that the first hump may be shifted to slightly higher energies by the presence of a less stable isomer. The prediction of a second kite VEDE at 5.2 eV could be tested by experiments with photons of higher energies. The range of relative energy predictions in Fig. 1 is sufficiently wide to prohibit definitive judgments on the relevance of the ring isomer; more exact total energy calculations are needed.

A restoration of two separated peaks takes place in the $Al_3O_5H_4^-$ spectrum. Both bands have full width at half

maximum (FWHM) values of 0.4. The first band approximately spans the 3.0–3.6 eV range; the second band's range is approximately 3.5–4.0 eV. Inspection of the published spectra places the maxima at approximately 3.3 and 3.8 eV, respectively. These results are compatible with the data of Table II and suggest that the symmetric book isomer is represented in the $Al_3O_5H_4^-$ spectrum.

Qualitative resemblances between $Al_3O_3^-$ and $Al_3O_5H_4^-$ spectra have their counterparts in the calculated VEDEs and Dyson orbitals of the book and symmetric book isomers of these anions. The absence of low-energy features implies that the second most stable isomer of Fig. 3 is not produced in the same experiment. Relative energies for the other isomers eliminate them from further consideration.

VI. CONCLUSIONS

The most stable form of $Al_3O_4H_2^-$ differs from the book form of $Al_3O_3^-$ by protonation of a noncentral oxide and by attachment of a hydroxide to the central aluminum, where the greatest positive charge resides. Each of the two lowest VEDEs of the resulting $Al_3O_4H_2^-$ cluster corresponds to a Dyson orbital localized on one of the noncentral aluminum atoms. A slightly less stable isomer of $Al_3O_4H_2^-$ may make minor contributions to the anion photoelectron spectrum. This structure differs from the kite form of $Al_3O_3^-$ by protonation of a bridging oxygen atom and by coordination of a hydroxide ligand to the central aluminum, which exhibits the highest positive charge in the precursor anion. The Dyson orbital for the lowest VEDE is localized on the two-coordinate aluminum atom and its counterpart for the second VEDE is localized on the one-coordinate aluminum atom. In the neutral cluster, the equilibrium geometry of the most stable isomer resembles that of the book form of $Al_3O_4H_2^-$. These anionic clusters are approximately 35 kcal/mol lower than the most stable $Al_3O_3^-(H_2O)$ complexes.

The addition of a second water molecule produces a book structure for $Al_3O_5H_4^-$ with two protonated, noncentral oxides and two hydroxide ligands attached to the central aluminum atom. Dyson orbitals for the first two VEDEs consist principally of antisymmetric and symmetric combinations of 3*s* functions on the noncentral aluminum atoms. These orbitals strongly resemble the Dyson orbitals for the first two VEDEs of the book form of $Al_3O_3^-$.

These results account for the similarity between the anion photoelectron spectra of $Al_3O_3^-$ and $Al_3O_5H_4^-$ (Ref. 8). Despite the absence of formal symmetry in the latter anion's minimum energy structure, the Dyson orbitals exhibit the delocalization that obtains in species with higher point-group symmetry. The electrostatic inequivalence of the two noncentral aluminum sites and the resulting localization of the Dyson orbitals are responsible for the contrasting anion photoelectron spectrum of $Al_3O_4H_2^-$.

The results of a computational study, recently submitted for publication and privately communicated to us, have reached similar conclusions on the most stable structures of $Al_3O_4H_2^-$ and $Al_3O_5H_4^-$ (Ref. 19).

ACKNOWLEDGMENTS

The authors would like to acknowledge Sara Jiménez Cortés, María Teresa Vázquez, and Dr. Srikanth Kambalapalli for technical support and DGSCA/UNAM (México) for providing computer time. This work was partially funded by DGAPA (Grant No. IN107399) and CONACYT-NSF (Grant No. E120.1778/2001). J.V.O. acknowledges support from the National Science Foundation through Grant No. CHE-0135823. We thank Professor Caroline Jarrold of Indiana University for sending an advance copy of Ref. 19.

[1] G. E. Brown, V. E. Henrich, W. H. Casey *et al.*, Chem. Rev. **99**, 77 (1999).
[2] J. R. Scott, G. S. Groenewold, A. K. Gianotto, M. T. Benson, and J. B. Wright, J. Phys. Chem. A **104**, 7079 (2000).
[3] S. B. H. Bach and S. W. McElvany, J. Phys. Chem. **95**, 9091 (1991).
[4] S. R. Desai, H. Wu, and L. S. Wang, Int. J. Mass Spectrom. Ion Processes **159**, 75 (1996).
[5] S. R. Desai, H. Wu, C. M. Rohlfing, and L. S. Wang, J. Chem. Phys. **106**, 1309 (1997).
[6] H. Wu, X. Li, X. B. Wang, C. F. Ding, and L. S. Wang, J. Chem. Phys. **109**, 449 (1998).
[7] F. A. Akin and C. C. Jarrold, J. Chem. Phys. **118**, 1773 (2003).
[8] F. A. Akin and C. C. Jarrold, J. Chem. Phys. **118**, 5841 (2003).
[9] G. Meloni, M. J. Ferguson, and D. M. Neumark, Phys. Chem. Chem. Phys. **5**, 4073 (2003).
[10] D. van Heijnsbergen, K. Demyk, M. A. Duncan, G. Meijer, and G. von Helden, Phys. Chem. Chem. Phys. **5**, 2515 (2003).
[11] E. F. Archibong and S. St-Amant, J. Phys. Chem. A **103**, 1109 (1999).
[12] T. K. Ghanty and E. R. Davidson, J. Phys. Chem. A **103**, 2867 (1999).
[13] T. K. Ghanty and E. R. Davidson, J. Phys. Chem. A **103**, 8985 (1999).
[14] A. Martínez, F. J. Tenorio, and J. V. Ortiz, J. Phys. Chem. A **105**, 8787 (2001).
[15] A. Martínez, F. J. Tenorio, and J. V. Ortiz, J. Phys. Chem. A **105**, 11291 (2001).
[16] A. Martínez, L. E. Sansores, R. Salcedo, F. J. Tenorio, and J. V. Ortiz, J. Phys. Chem. A **106**, 10630 (2002).
[17] A. Martínez, F. J. Tenorio, and J. V. Ortiz, J. Phys. Chem. A **107**, 2589 (2003).
[18] X. Y. Cui, I. Morrison, and J. G. Han, J. Chem. Phys. **117**, 1077 (2002).
[19] F. A. Akin and C. C. Jarrold (private communication).
[20] (a) J. V. Ortiz, in *Computational Chemistry: Reviews of Current Trends*, edited by J. Leszczynski (World Scientific, Singapore, 1997), Vol. 2, p. 1; (b) Adv. Quantum Chem. **35**, 33 (1999); (c) J. V. Ortiz, V. G. Zakrzewski, and O. Dolgounitcheva, in *Conceptual Trends in Quantum Chemistry*, edited by E. S. Kryachko (Kluwer, Dordrecht, 1997), Vol. 3, p. 465.
[21] M. J. Frisch, G. W. Trucks, H. B. Schlegel *et al.*, GAUSSIAN 98, revision A8, Gaussian Inc., Pittsburg, PA, 1998.
[22] (a) A. D. Becke, J. Chem. Phys. **98**, 5648 (1993); (b) C. Lee, W. Yang, and R. G. Parr, Phys. Rev. B **37**, 785 (1988); (c) B. Mielich, A. Savin, H. Stoll, and H. Preuss, Chin. Phys. Lasers **157**, 200 (1989).
[23] (a) R. Krishnan, J. S. Binkley, R. Seeger, and J. A. Pople, J. Chem. Phys. **72**, 650 (1980); (b) T. Clark, J. Chandrasekhar, G. W. Spitznagel, and P. v. R. Schleyer, J. Comput. Chem. **4**, 294 (1983); (c) M. J. Frisch, J. A. Pople, and J. S. Binkley, J. Chem. Phys. **80**, 3265 (1984); (d) A. D. McLean and G. S. Chandler, *ibid.* **72**, 5639 (1980).
[24] J. V. Ortiz, J. Chem. Phys. **104**, 7599 (1996).
[25] A. M. Ferreira, G. Seabra, O. Dolgounitcheva, V. G. Zakrzewski, and J. V. Ortiz, in *Quantum-Mechanical Prediction of Thermochemical Data*, edited by J. Cioslowski (Kluwer, Dordrecht, 2001), p. 131.
[26] W. von Niessen, W. Schirmer, and L. S. Cederbaum, Comput. Phys. Rep. **1**, 57 (1984).
[27] V. G. Zakrzewski, J. V. Ortiz, J. A. Nichols, D. Heryadi, D. L. Yeager, and J. T. Golab, Int. J. Quantum Chem. **60**, 29 (1996).
[28] G. Schaftenaar, computer code MOLDEN 3.4, CAOS/CAMM Center, Nijmegen, The Netherlands.